IET Electric Power Applications

Research Article

IET Journals
The Institution of Engineering and Technology

Online maximum torque per power losses strategy for indirect rotor flux-oriented control-based induction motor drives

ISSN 1751-8660
Received on 4th July 2018
Revised 21st November 2018
Accepted on 5th December 2018
E-First on 22nd January 2019
doi: 10.1049/iet-epa.2018.5403
www.ietdl.org

Hossein Abootorabi Zarchi[1] ✉, *Hamidreza Mosaddegh Hesar*[1], *Mojtaba Ayaz Khoshhava*[1]

[1]*Department of Electrical Engineering, Faculty of Engineering, Ferdowsi University of Mashhad, Mashhad 91775-1111, Iran*

✉ *E-mail: abootorabi@um.ac.ir*

Abstract: Among the conventional loss minimisation algorithms (LMAs), the model-based approaches have the advantages of fast response and high accuracy. Here, a novel online model-based power losses minimisation approach is presented for indirect field-oriented control (IFOC) of induction motor (IM) drives. The proposed method is introduced as maximum torque per power losses (MTPPL) in which the power losses for a given torque are minimised. The results demonstrate that the proposed approach preserves the LMA merits, while the criterion for the MTPPL scheme is achieved. The mentioned criterion is investigated by a gradient approach so that while the gradient vectors of the torque and power losses are parallel, the MTPPL strategy is realised. The closed-loop IFOC of the MTPPL approach is implemented in real time for a laboratory 2.2 kW three-phase IM drive. The experimental results show the capability and validity of the proposed control scheme.

Nomenclature

$\boldsymbol{V}, \boldsymbol{I}, \boldsymbol{\psi}$	voltage, current, flux vectors
T_e	electromagnetic torque
R	winding resistance
R_i	iron loss resistance
L_l	leakage inductance
L_m	coupling inductance between stator and rotor
p	pole pair number of stator
ω_r	electrical rotor speed
ω	angular speed of rotor flux
$\omega_{slip} = \omega - \omega_r$	slip speed
$T_r = L_{lr}/R_r$	rotor time constant

Subscripts

s, r	stator and rotor
d, q	rotating direct and quadrature axes

1 Introduction

Generally, the most frequent type of electrical motors in the industry is three-phase induction ones, because they involve low maintenance costs and their operation is highly reliable [1]. Therefore, their electric energy consumption is of great importance. Furthermore, as the electric energy costs are augmented in recent years, consumers are more interested in high-efficient electric motors. Consequently, manufacturers have attempted to produce low-loss electric motors in recent years [2–4]. For instance, the application of IE1 type electric motors is reduced by 10% in the last 4 years [5]. The efficiency improvement in design and manufacturing process is taken into account just according to the nominal condition operation. As a result, the power losses will be relatively high in light load and variable speed applications, even if a high-efficient electric motor is used [6]. The main reason of efficiency reduction in electric motors when keeping out the nominal operating point is the imbalance between the copper and iron losses, which are the two main components of the power losses in an electromotor. Accordingly, the application of high-efficient control schemes for electric motors is substantial.

Most of the suggested methods for efficiency improvement in non-nominal operating condition select the optimal flux value and re-establish the balance between copper and iron losses. Generally, there are two main approaches for efficiency optimisation in AC motor drives: model-based and search-based methods [7]. In the model-based methods, the motor loss model is derived and a loss minimisation strategy is realised on the derived model [8–18]. These methods are easy to implement, but they require the exact machine parameters. Therefore, the parameters variation during various operating conditions may lead to non-optimal operation. Other methods are independent of true motor parameters and load conditions and they could be implemented on any type of electrical motors and control schemes [19–22]. Indeed, a search-based algorithm should be fast enough to respond to load variations. In this approach, a control parameter, which could be the reference flux magnitude, is varied step by step until the input power is minimised for a desired load torque and rotor speed. Consequently, continuously tuning the control parameters results in online loss power minimisation. Actually, in this case, the motor input power is selected as the objective function (OF) and the reference flux magnitude is determined by a search algorithm according to this OF. In this technique, if a disturbance or a sudden and unexpected change is occurred in the mechanical load, the reference flux should be accordingly changed, otherwise, instability may occur in the motor drive system. Therefore, the flux search-based algorithms could be confidentially applied only if the mechanical load variations pattern is definite.

In addition to the two above-mentioned methods, hybrid methods are proposed in recent years [23, 24]. The hybrid methods are faster than search-based algorithms and their sensitivity to the machine parameters is low in comparison to model-based methods [25]. This paper belongs to the model-based category.

In the model-based algorithms, to ensure realising the efficiency optimisation, the loss minimisation factor is usually obtained by differentiating the power losses with respect to variables like d-axis stator current [9], rotor flux [13], d and q-axis stator current [17], and slip speed [18].

In the strategy proposed in [8], the direct and quadrature axis power losses are forced to be equal through proportional–integral (PI) to minimise the power losses. However, due to the presence of harmonics in the power losses components, tuning the PI gains is very complicated. In [9], the induction motor (IM) total losses is derived as a function of the stator current. The differentiation of the loss expression with respect to d-axis stator current gives the optimal magnetising current. However, the iron loss which is highly dependent on the frequency variations is considered constant in all operation conditions.

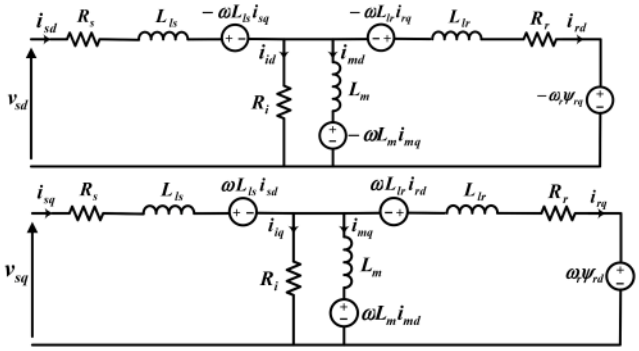

Fig. 1 *d–q-axis equivalent circuit of an IM in rotor flux reference frame considering iron loss*

In [10], the motor electrical loss function is calculated and its gradient respect to the rotor flux is equalised to zero to determine the optimal flux orthogonal components. The rotor current reference values are calculated according to the optimal flux and reference rotor speeds. A loss minimisation strategy applicable both in steady-state and transient conditions is proposed in [11]. In the proposed strategy, the magnetising inductance variation is taken into account. However, the iron losses, which can be a considerable portion of the total losses, especially in saturation condition, are neglected.

In [12], the optimal relation between d and q-axis stator currents is achieved by differentiating the loss function with respect to the d-axis stator current based on a simplified IM model considering iron loss. In [13], a steady-state loss model including both the motor and inverter losses for linear IM (LIM) drive has been introduced in terms of rotor flux. The optimal flux that leads to the minimum loss of LIM is assigned by setting the derivative of loss function to zero.

Sridharan and Krein [14] have applied loss minimisation on a combination of IM and inverter losses. In this paper, to ensure the total losses minimisation using a comprehensive loss model, a system-level loss minimisation approach is developed. System-level strategies minimise the total losses, e.g. losses in the machine, filter, inverter, and its DC-link. In [15], the proportion of the d and q-axis of the magnetising current is controlled such that the machine electrical losses be minimised. The proposed strategy is complicated and not easy to implement in practical applications.

A strategy to improve the ride-through capability of an inverter fed IM is proposed in [16]. The ride-through duration is increased through loss minimisation. The proposed loss minimisation uses various look-up tables in order to take into account parameter variation in different rotor speeds which complicates its practical implementation. In [17], the loss minimisation criterion is achieved through differentiation of the total loss function with respect to d and q-axis stator current. This reference disregards the iron loss resistance in the torque equation which certainly deviates true loss minimisation implementation.

In this paper, the indirect field-oriented control (FOC) in the rotor flux reference frame is applied in combination with the MTPPL strategy for a three-phase IM drive. Despite the strategy proposed in [17], in our strategy, the d and q-axis stator currents relationship is derived using the gradient method considering the iron loss and without any approximation. It should be mentioned that the iron loss negligence deteriorates the operation of the FOC of IM drive [26]. Consequently, in this research, a rotor-flux estimator is used to overcome detuning issue.

The detailed description of the proposed loss minimisation strategy and control system will be done in the following sections; Section 2 describes the IM model including iron loss. In Section 3, the criterion for the MTPPL scheme is introduced. In Section 4, the experimental results are presented. Finally, Section 5 contains the concluding remarks.

2 Induction motor model including iron loss

An iron loss version of the IM model is shown in Fig. 1. The d–q-axis dynamic model of IM in the rotor-flux reference frame is described as [27]

$$v_{sd} = R_s i_{sd} + \mathrm{d}\psi_{sd}/\mathrm{d}t - \omega\psi_{sq} \tag{1}$$

$$v_{sq} = R_s i_{sq} + \mathrm{d}\psi_{sq}/\mathrm{d}t + \omega\psi_{sd} \tag{2}$$

$$v_{rd} = 0 = R_r i_{rd} + \mathrm{d}\psi_{rd}/\mathrm{d}t - (\omega - \omega_r)\psi_{rq} \tag{3}$$

$$v_{rq} = 0 = R_r i_{rq} + \mathrm{d}\psi_{rq}/\mathrm{d}t + (\omega - \omega_r)\psi_{rd} \tag{4}$$

$$\psi_{sd} = L_{ls} i_{sd} + L_m i_{md} \quad \psi_{sq} = L_{ls} i_{sq} + L_m i_{mq} \tag{5}$$

$$\psi_{rd} = L_{lr} i_{rd} + L_m i_{md} \quad \psi_{rq} = L_{lr} i_{rq} + L_m i_{mq} \tag{6}$$

$$\begin{aligned} R_i i_{id} &= L_m \mathrm{d}i_{md}/\mathrm{d}t - \omega L_m i_{mq} \\ R_i i_{iq} &= L_m \mathrm{d}i_{mq}/\mathrm{d}t + \omega L_m i_{md} \end{aligned} \tag{7}$$

$$T_e = \frac{3p}{2}(L_m/L_r)\left(\psi_{rd}(i_{sq} - i_{iq}) - \psi_{rq}(i_{sd} - i_{id})\right) \tag{8}$$

The rotor flux-oriented control is defined with the following constraints

$$\psi_{rd} = |\boldsymbol{\psi}_r| \quad \psi_{rq} = 0 \tag{9}$$

Considering the constraints given by (9), the rotor voltage equations expressed in the rotor flux-oriented reference frame can be used to obtain the rotor magnetising current space vector ($\boldsymbol{i}_m$) and slip speed (ω_{slip}).

Substitution of (6) into (3) and (4) yields the following rotor voltage differential equation

$$0 = \frac{R_r}{L_{lr}}\boldsymbol{\psi}_r - \frac{R_r L_m}{L_{lr}}\boldsymbol{i}_m + \frac{\mathrm{d}\boldsymbol{\psi}_r}{\mathrm{d}t} + j\omega_{slip}\boldsymbol{\psi}_r \tag{10}$$

By decomposing into real and imaginary-axis components, the following equations are obtained which describe the flux model in the rotor flux-oriented reference frame

$$0 = \frac{R_r}{L_{lr}}|\boldsymbol{\psi}_r| - \frac{R_r L_m}{L_{lr}} i_{md} + \frac{\mathrm{d}|\boldsymbol{\psi}_r|}{\mathrm{d}t} \Rightarrow L_m i_{md} = |\boldsymbol{\psi}_r| + T_r \frac{\mathrm{d}|\boldsymbol{\psi}_r|}{\mathrm{d}t} \tag{11}$$

$$0 = -\frac{R_r L_m}{L_{lr}} i_{mq} + \omega_{slip}|\boldsymbol{\psi}_r| \Rightarrow \omega_{slip} = \frac{L_m}{T_r|\boldsymbol{\psi}_r|} i_{mq} \tag{12}$$

In the rotor flux-oriented control, by taking iron loss into account, the output torque is conveniently described as

$$T_e = \left(\frac{1}{\beta^2 + 1}\right) \cdot \left(\frac{R_i}{\omega L_{lr}}\right)\left(\beta\, i_{sq}\psi_{rd} - i_{sd}\psi_{rd} - \frac{\psi_{rd}^2}{L_{lr}}\right) \tag{13}$$

where $\beta = (R_i/\omega L_{lr}) + (R_i/\omega L_m)$.

To determine the MTPPL realisation criterion, the torque expression will be rewritten to an appropriate form, in the next section.

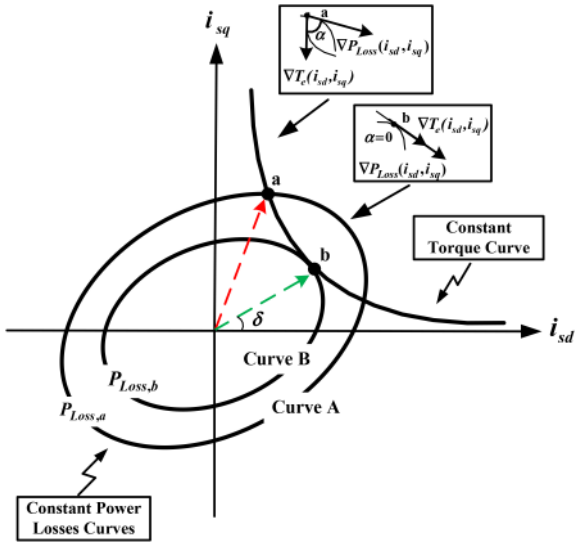

Fig. 2 *Constant torque curve and power losses curves*

3 Loss minimisation algorithm

In this paper, the realisation of IM power losses minimisation strategy is considered under the constraint of constant load torque. Accordingly, the power losses are selected as the OF, which is to be minimised. Based on Lagrange's theorem, it can easily be claimed that the control strategy is realised when the torque curve and the considered OF are tangent at a point, or, in other words, their gradient vectors are parallel. The efficiency optimisation approach is achieved by minimising power losses under the condition of constant output power. In order to obtain the loss minimisation strategy based on Lagrange's theorem, the torque and power losses expressions including iron loss must be written based on the two-axis terminal stator currents. In the following, the mentioned procedures are presented in detail.

3.1 Derivation of electromagnetic torque

In the rotor flux-oriented control, the torque equation is given by (13). From (7) and writing i_{md} in terms of i_{iq}, we have

$$i_{md} = \frac{R_i i_{iq}}{\omega L_m} \tag{14}$$

Substituting (14) into (6) gives (15)

$$\psi_{rd} = L_{ls} i_{rd} + L_m \left(\frac{R_i}{\omega L_m} i_{iq} \right) \tag{15}$$

Considering $i_{rd} = i_{md} + i_{id} - i_{sd}$, (15) is rewritten as

$$\begin{aligned} & i_{rd} = \frac{R_i}{\omega L_m} i_{iq} + \left(\frac{1}{1+\beta^2} \right) \left(i_{sd} + \frac{\psi_{rd}}{L_{lr}} - \beta i_{sq} \right) - i_{sd} \\ & \Downarrow \\ & \psi_{rd} = \frac{R_i}{\omega} \left(1 + \frac{L_{lr}}{L_m} \right) i_{iq} + L_{lr} \left(\frac{1}{1+\beta^2} - 1 \right) i_{sd} - \frac{\beta L_{lr}}{1+\beta^2} i_{sq} + \frac{\psi_{rd}}{1+\beta^2} \end{aligned} \tag{16}$$

Considering $i_{iq} = i_{sq} + \beta i_{sd} + \beta \psi_{rd} / L_{lr}$ and after a few manipulation, (13) is developed as

$$T_e = \left(\frac{\beta^2 - 1}{\beta^2 + 1} \right) \cdot \left(\frac{R_i}{\beta \omega} \right) \left(i_{sq} i_{sd} - \frac{i_{sq}^2}{\beta} \right) \tag{17}$$

3.2 Derivation of electrical power losses

As the windage and friction losses in an IM for a desired rotor speed and load torque are independent of the stator current [9], the stator reference current is determined regarding only the copper and iron losses. The electrical power losses consist of the following components

$$P_{cu,s} = R_s (i_{sd}^2 + i_{sq}^2) \tag{18}$$

$$P_{cu,r} = R_r i_{rq}^2 = R_r \left(\frac{R_i}{R_r + R_i} i_{sq} - \frac{\omega_r L_m}{R_r + R_i} i_{sd} \right)^2 \tag{19}$$

$$P_{iron} = R_i i_{iq}^2 = R_r (i_{sq} - i_{rq})^2 \tag{20}$$

where $P_{cu,s}$ is the stator copper loss, $P_{cu,r}$ the rotor copper loss, and P_{iron} the iron loss. Substituting

$$i_{rq} = \left(\frac{R_i}{R_r + R_i} \right) i_{sq} - \left(\frac{\omega_r L_m}{R_r + R_i} \right) i_{sd}$$

into (20) gives (21)

$$P_{iron} = R_r \left(\frac{R_r}{R_r + R_i} i_{sq} + \frac{\omega_r L_m}{R_r + R_i} i_{sd} \right)^2 \tag{21}$$

So, the electrical power losses can be expressed as

$$P_{Loss} = \underbrace{\left(R_s + \frac{\omega_r^2 L_m^2}{R_r + R_i} \right)}_{K_d} i_{sd}^2 + \underbrace{\left(R_s + \frac{R_r R_i}{R_r + R_i} \right)}_{K_q} i_{sq}^2 \tag{22}$$

3.3 MTPPL strategy

In this section, the minimisation of (22) is selected as OF under a given load torque. According to (17), the torque equation for rotor FOC (considering the iron loss) can be drawn on the $i_{sd} - i_{sq}$ plane. On the same plane, a curve representing the power losses takes the form of an ellipse (22). Under the constraint of constant torque, if an operating point is set at point '*a*' in Fig. 2, the curve A is supposed to be constant power losses curve ($P_{Loss,a}$). If an operating point is set at '*b*', the curve B is another constant power losses curve ($P_{Loss,b}$).

Using Lagrange's theorem, it can be easily found that the power losses are minimum when the torque curve and the power losses curve are tangent at a point if and only if their gradient vectors are parallel at the point of tangency (see '*b*' in Fig. 2), so that

$$\| \nabla T_e(i_{sd}, i_{sq}) \| \| \nabla P_{Loss}(i_{sd}, i_{sq}) \| \sin \alpha = 0 \tag{23}$$

where α is the angle between $\nabla T_e(i_{sd}, i_{sq})$ and $\nabla P_{Loss}(i_{sd}, i_{sq})$. Therefore, the criterion of MTPPL strategy realisation is obtained as follows:

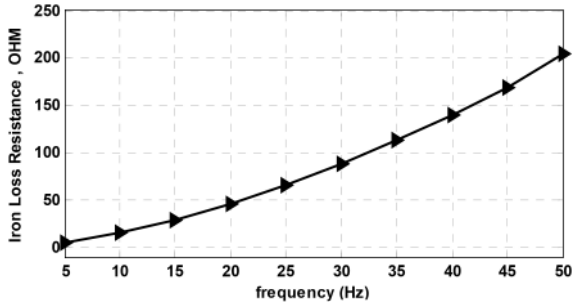

Fig. 3 *Identified values of equivalent iron loss resistance for the 2.2 kW IM*

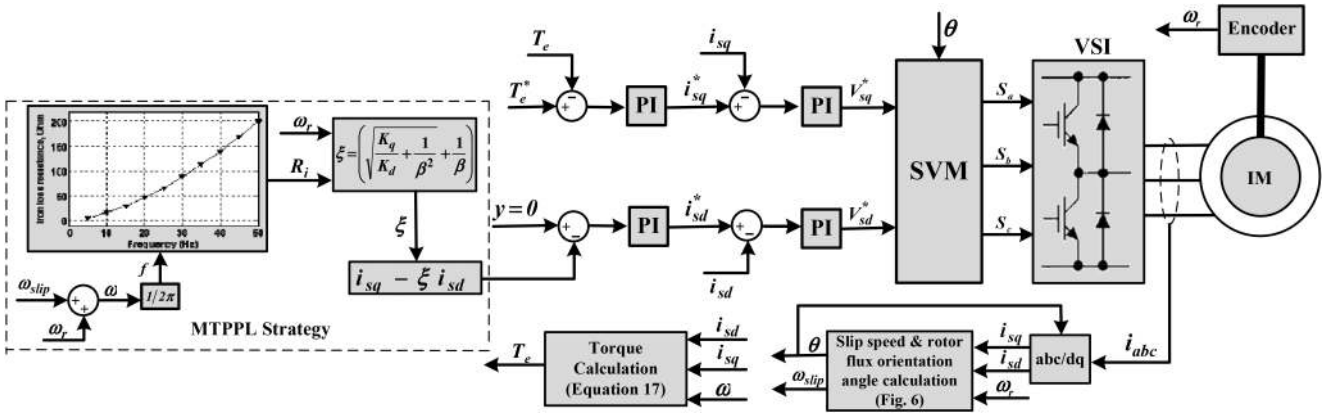

Fig. 4 *Proposed online MTPPL control strategy for rotor flux-oriented control-based IM drives*

$$y = \| \nabla T_e(i_{sd}, i_{sq}) \| \| \nabla P_{Loss}(i_{sd}, i_{sq}) \| \sin\alpha \tag{24}$$

It is obvious that the control strategy is realised when y is kept at zero. The cross-product of gradient vectors is calculated from the following equation

$$\nabla T_e(i_{sd}, i_{sq}) \times \nabla P_{Loss}(i_{sd}, i_{sq}) = \det \begin{bmatrix} i & j & k \\ \frac{\partial T_e}{\partial i_{sd}} & \frac{\partial T_e}{\partial i_{sq}} & 0 \\ \frac{\partial P_{Loss}}{\partial i_{sd}} & \frac{\partial P_{Loss}}{\partial i_{sq}} & 0 \end{bmatrix} \tag{25}$$

So, the criterion of MTPPL realisation is achieved as follows:

$$\begin{aligned} y &= \frac{\partial T_e}{\partial i_{sd}} \times \frac{\partial P_{Loss}}{\partial i_{sq}} - \frac{\partial T_e}{\partial i_{sq}} \times \frac{\partial P_{Loss}}{\partial i_{sd}} = 0 \\ &= K_q i_{sq}^2 - K_d i_{sd}^2 + \frac{2K_d i_{sq} i_{sd}}{\beta} = 0 \\ &= \left(\frac{K_q}{K_d} + \frac{1}{\beta^2}\right) i_{sq}^2 - \left(i_{sd} - \frac{1}{\beta} i_{sq}\right)^2 = 0 \Rightarrow i_{sd} = \left(\sqrt{\frac{K_q}{K_d} + \frac{1}{\beta^2}} + \frac{1}{\beta}\right) i_{sq} \end{aligned} \tag{26}$$

The locus of stator current for maximum torque per ampere strategy is a straight line at $\delta = \pm \pi/4$, if iron losses are neglected. In the non-ideal condition, δ is smaller than $\pi/4$ dependent on the R_i value. For MTPPL, the minimum power losses are realised at a point depended on the iron loss resistance and the rotor speed. Accordingly, the stator current angle can be less or > $\pi/4$ dependent on rotor speed [7]. By doing some calculations on (26), we have

$$i_{sd} = i_{sq}\,\xi \Rightarrow \delta = \tan^{-1}(1/\xi) \tag{27}$$

where

$$\xi = \left(\sqrt{\frac{K_q}{K_d} + \frac{1}{\beta^2}} + \frac{1}{\beta}\right).$$

3.4 Measurement of iron loss resistance R_i

According to Fig. 3, experimentally identified equivalent iron loss resistance values of the 2.2 kW IM can be acquired by measuring the input power at a no-load test. Although R_i varies with the operating frequency and the flux level, it is more sensitive to the variation of frequency rather than the rotor flux variations [28, 29].

4 Experimental set-up and results

The overall block diagram of the proposed drive system is shown in Fig. 4. The performance of the proposed system is evaluated through a digital signal processor (DSP)-based prototype system. The experimental set-up is shown in Fig. 5 consists of: a 2.2 kW IM, a 3 kW DC generator with an external rheostat in the armature terminal as a generator load, a voltage source inverter with corresponding driver board, a sensor board, and a TMS320F28335 signal processor board designed with Texas Instrument Co. The rotor speed is measured by a 1024 pulses incremental encoder mounted on the IM shaft. The stator phase currents are measured using two Hall-effect current sensors (LEM LTS-6-NP) and the line-to-line voltages are detected by voltage sensors (LEM LV-25-P). The experimental set-up is also equipped with an analogue second-order low-pass filters with 2.6 kHz cut-off frequency for filtering the measured stator current and voltage signals. The inverter consists of insulated-gate bipolar transistor (IGBT) module SKM40GD124D (with 40 A, 1200 V ratings) and HCPL 316 J type intelligent IGBT drivers. These kind of IGBT drivers provide electrical isolation between the power and control systems. The switching frequency is selected 10 kHz for the inverter. In order to shoot through protection of inverter switches, the dead-time is 1 μs. It should be noted that the set-up is designed completely modular and the supply voltage for each of the boards is 24 V DC. The calculated variables in the DSP are shown on the oscilloscope using the digital analogue converter-pulse-width modulation output of DSP. Indeed, the PWM value of the variable is converted to an analogue data through a low-pass filter.

Table 1 shows the specifications and parameters of the 2.2 kW IM and the PI controller gains are illustrated in Table 2. In the proposed control approach, a first-order model of the plant is used to design PI controllers. In vector control, the PI controller parameters are regulated based on transfer function of the stator *d*–

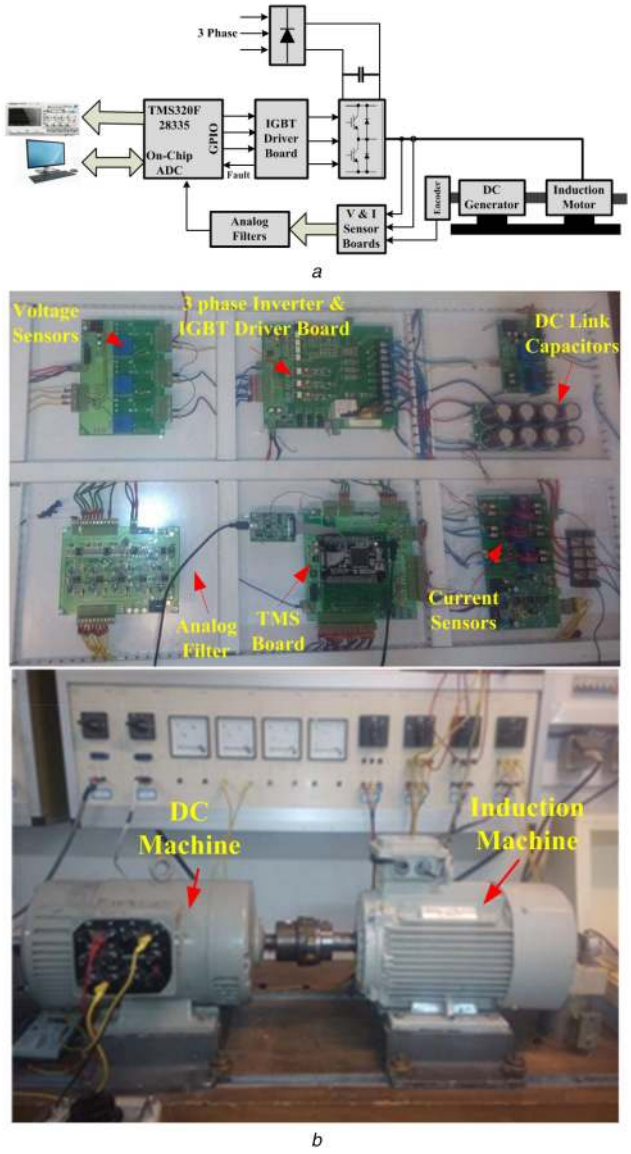

Fig. 5 *Experimental set-up*
(a) Laboratory implementation block diagram, ***(b)*** IM drive system hardware

Table 1 IM parameters

Parameter	Value	Parameter	Value
rated power, kW	2.2	L_m, H	0.1863
pole-pair	2	L_{ls}, H	0.047
rated voltage, *V*	180	R_r^P, Ω	1.1237
R_s, Ω	1.3012	L_{lr}^P, H	0.0206

Table 2 PI controller gains

	Proportional gain (K_p)	Integral gain (K_i)
MTPPL	7	0.5
d-axis current control	0.08	0.5
q-axis current control	0.08	0.5
torque control	5	4

q currents to the stator voltages (control inputs). Therefore, the IM model is converted into a single-input, single-output model. As a result, the conventional design methods for first-order control systems are applicable.

The slip speed (ω_{slip}) calculation is necessary for MTPPL strategy. Since the value of i_{mq} is not measurable, it is impossible to use (12). To solve this problem, a block diagram is derived considering (6) and (7) which is shown in Fig. 6. This scheme is

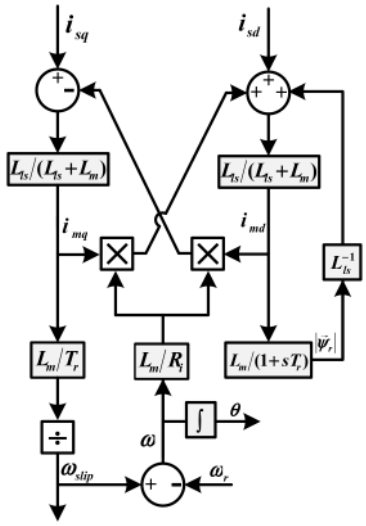

Fig. 6 *Slip speed and rotor flux orientation angle calculation considering iron loss*

applicable for flux rotor estimation with iron loss compensation. In this estimator, by measuring the stator current and rotor speed, the slip speed and the rotor flux orientation angle (θ) are calculated.

The experimental results of the proposed control approach based on indirect FOC are illustrated in Figs. 7–9. As shown, in both transient and steady-state conditions, the MTPPL realisation criterion tracks its reference value and the strategy is realised (Fig. 7*a*). Fig. 7*b* represents that the torque tracks a repeating sequence step command of reference, properly. As a result, the rotor speed increases and decreases rather linearly as shown in Fig. 7*c*. The two-axis stator current components are illustrated in Figs. 7*d* and *e*. According to Fig. 3, the variation of operating frequency changes the R_i value. As shown in Fig. 7*f*, along with the speed variation and consequently frequency variation, ξ is determined by (27).

Figs. 8*a* and *b* show the input power of the IM with and without the proposed strategy. In this condition, the rotor speed is controlled at 500 rpm and the load torque is changed between 2 and 6 N m, periodically. It can be seen that at the same load torque and speed, the input power under the MTPPL control method considerably reduces in comparison with the constant flux method. The reduction in input power for $T_l = 2$ Nm and $T_l = 6$ Nm is ~ 22.5 and 14.7%, respectively. To investigate the overall operation of the proposed LMA at different rotor speeds and torques, the IM drive is controlled for $n_r = 500$, 1000 rpm at various torque from light to nominal load (Fig. 9). The results verify the effectiveness of the presented strategy at different conditions. As expected, the input power reduction is more significant in light load condition. In order to compare the proposed LMA with other power losses minimisation strategies, Table 3 summarises the improvements caused by some of the LMAs available in the literature. To fair comparison, only the papers are studied in which the standard IMs with the power ratings in the range of 1.5–3 kW were used. In this table, the announced results are the average values for power losses reduction, input power reduction, and efficiency improvement for different load torques.

The model-based LMAs are expected to drift from the optimum with parameter variation [25]. To evaluate the sensitivity of the proposed strategy realisation to the motor parameters variation, the efficiency sensitivity due to R_i, R_s, and L_m is shown in Fig. 10. The results are related to $T_l = 5$ Nm and $n_r = 500$ rpm. The conclusion which can be achieved from this plot is that efficiency is more sensitive to error in the L_m compared to R_i and R_s. Therefore, for reasonable performance under all operating conditions, an exact estimate of L_m is required. If the value of R_s is known with an accuracy of ±50%, the efficiency changes will not be too great. This means that the R_s estimator does not need to have high accuracy to realise the proposed strategy.

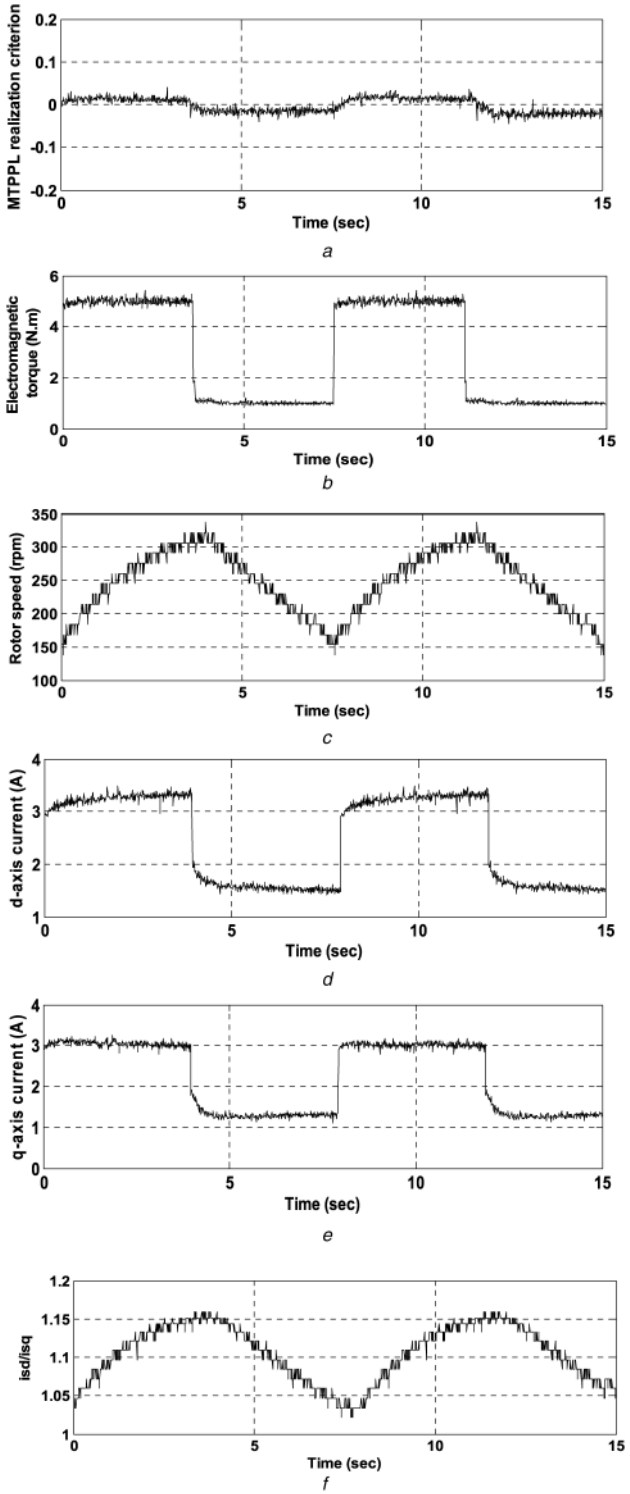

Fig. 7 *Experimental results of MTPPL control for IM drive system*

5 Conclusion

In this paper, an indirect FOC algorithm was merged with online MTPPL control for IM drives. Under the constraint of constant torque, the proposed approach minimised the power losses of the IM, i.e. copper and iron losses. By controlling the power losses minimisation criterion directly, the proposed scheme can optimise the efficiency of the IM without deteriorating the dynamics performance. Furthermore, the iron loss impact, as a cause of detuned operation of the rotor flux orientation, was discussed. As a result, a rotor flux estimator was used that operates on the basis of measurement of stator currents and rotor speed. To prove the usefulness of the proposed control approach, a real-time implementation was carried out where the excellent performance of the presented method could be verified.

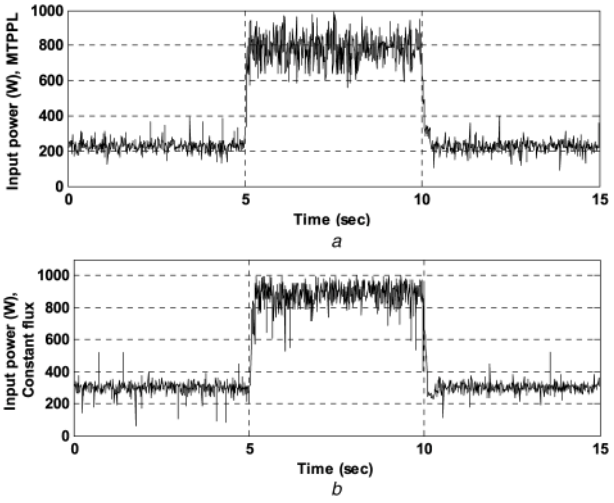

Fig. 8 *Input power of IM drive*
(a) With the proposed strategy, ***(b)*** With the constant flux

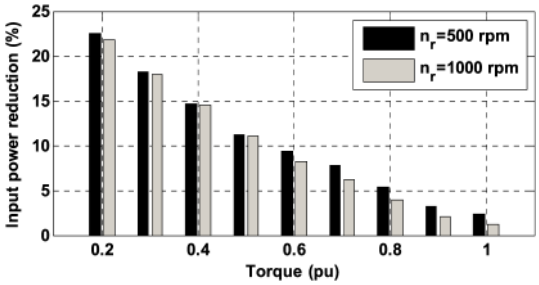

Fig. 9 *Input power reduction with load torque changes*

Table 3 Summary of LMAs performance in the literature

Ref.	Motor rating, kW	Type of strategy	Improvement
[13]	3	model based	controllable[a] losses reduced by 4.6%
[29]	2.2	model based	efficiency improved by 8.676%
[30]	2.2	model based	input power reduced by 4.35%
[31]	1.5	model based	efficiency improved by 6.79%
proposed approach	2.2	model based	input power reduced by 10.22%

[a]The copper and iron losses are controllable losses.

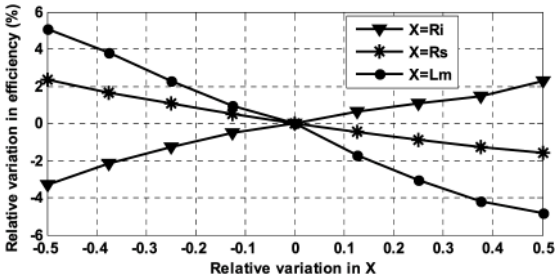

Fig. 10 *Sensitivity of efficiency to variation in R_i, R_s, and L_m*

6 Acknowledgment

The authors wish to express appreciation to Research Deputy of Ferdowsi University of Mashhad for supporting this project by grant no. 47319 (22 July 2018).

7 References

[1] Almeida, A.T., Ferreira, F.J.T.E., Baoming, G.: 'Beyond induction motors – technology trends to move-up efficiency', *IEEE Trans. Ind. Appl.*, 2014, **50**, (3), pp. 2103–2114

[2] Ferreira, F.J.T.E., Baoming, G., Almeida, A.T.: 'Reliability and operation of high-efficiency induction motors', *IEEE Trans. Ind. Appl.*, 2016, **52**, (6), pp. 4628–4637

[3] Malinowski, J., McCormick, J., Dunn, K.: 'Advances in construction techniques of AC induction motors: preparation for super-premium efficiency levels', *IEEE Trans. Ind. Appl.*, 2004, **40**, (6), pp. 1665–1670

[4] Kirtley, J.L., Cowie, J.G., Brush, E.F.*, et al.*: 'Improving induction motor efficiency with die-cast copper rotor cages'. IEEE Power Engineering Society General Meeting, Tampa, FL, USA, 2007, pp. 1–6

[5] Chausovsky, A.: 'Motor market update', Presentation Slides, Zurich, 2014

[6] Gnacinski, P., Tarasiuk, T.: 'Energy-efficient operation of induction motors and power quality standards', *Electr. Power Syst. Res.*, 2016, **135**, pp. 10–17

[7] Kirschen, D.S., Novotny, D.W., Lipo, T.A.: 'On-line efficiency optimization of a variable frequency induction motor drive', *IEEE Trans. Ind. Appl.*, 1985, **IA-21**, (4), pp. 610–616

[8] Abrahamsen, F., Blaabjerg, F., Pedersen, J.K.*, et al.*: 'On the energy optimized control of standard and high-efficiency induction motors in CT and HVAC applications', *IEEE Trans. Ind. Appl.*, 1998, **34**, (4), pp. 822–831

[9] Uddin, M.N., Nam, S.W.: 'New online loss-minimization-based control of an induction motor drive', *IEEE Trans. Power Electron.*, 2008, **23**, (2), pp. 926–933

[10] Domínguez, J.R., Mora-Soto, C., Ortega-Cisneros, S.*, et al.*: 'Copper and core loss minimization for induction motors using high-order sliding-mode control', *IEEE Trans. Ind. Electron.*, 2012, **59**, (7), pp. 2877–2889

[11] Borisevich, A., Schullerus, G.: 'Energy efficient control of an induction machine under torque step changes', *IEEE Trans. Energy Convers.*, 2016, **14**, (8), pp. 1295–1303

[12] Li, J., Xiao, F., Zhang, S.: 'Simplified loss model control efficiency optimization algorithm for vector control induction motor drives'. 43rd Annual Conf. of the Industrial Electronics Society (IECON), Beijing, China, 2017, pp. 5178–5183

[13] Hu, D., Xu, W., Dian, R.*, et al.*: 'Loss minimization control of linear induction motor drive for linear metros', *IEEE Trans. Ind. Electron.*, 2018, **65**, (9), pp. 6870–6880

[14] Sridharan, S., Krein, P.T.: 'Minimization of system-level losses in VSI-based induction motor drives: offline strategies', *IEEE Trans. Ind. Appl.*, 2017, **53**, (2), pp. 1096–1105

[15] Yu, J., Pei, W., Zhang, Ch.: 'A loss-minimization port-controlled Hamilton scheme of induction motor for electric vehicles', *IEEE/ASME Trans. Mechatronics*, 2015, **20**, (6), pp. 2645–2653

[16] Titus, J., Teja, J., Hatua, K.*, et al.*: 'An improved scheme for extended power loss ride-through in a voltage source inverter fed vector controlled induction motor drive using a loss minimization technique', *IEEE Trans. Ind. Appl.*, 2016, **52**, (2), pp. 1500–1508

[17] Garcia, G.O., Mendes Luis, J.C., Stephan, R.M.*, et al.*: 'An efficient controller for an adjustable speed induction motor drive', *IEEE Trans. Ind. Electron.*, 1994, **41**, (5), pp. 533–539

[18] Mannan, A., Murata, T., Tamura, J.*, et al.*: 'Efficiency optimized speed control of field oriented induction motor including core loss'. Proc. of the Power Conversion Conf., Osaka, Japan, 2002, pp. 1316–1321

[19] Kaboli, Sh., Zolghadri, M.R., Vahdati-Khajeh, E.: 'A fast flux search controller for DTC-based induction motor drives', *IEEE Trans. Ind. Electron.*, 2007, **54**, (5), pp. 2407–2416

[20] Hajian, M., Arab Markadeh, G.R., Soltani, J.*, et al.*: 'Energy optimized sliding-mode control of sensorless induction motor drives', *Energy Convers. Manage.*, 2009, **50**, (9), pp. 2296–2306

[21] Bašić, M., Vukadinović, D.: 'Online efficiency optimization of a vector controlled self-excited induction generator', *IEEE Trans. Energy Convers.*, 2016, **31**, (1), pp. 373–380

[22] Shreelakshmi, M.P., Agarwal, V.: 'Trajectory optimization for loss minimization in induction motor fed elevator systems', *IEEE Trans. Power Electron.*, 2018, **33**, (6), pp. 5160–5170

[23] Chakraborty, C., Hori, Y.: 'Fast efficiency optimization techniques for the indirect vector-controlled induction motor drives', *IEEE Trans. Ind. Appl.*, 2003, **39**, (4), pp. 1070–1076

[24] Vukosavic, S.N., Levi, E.: 'Robust DSP-based efficiency optimization of a variable speed induction motor drive', *IEEE Trans. Ind. Electron.*, 2003, **50**, (3), pp. 560–570

[25] Bazzi, A.M., Krein, P.T.: 'Review of methods for real-time loss minimization in induction machines', *IEEE Trans. Ind. Appl.*, 2010, **46**, (6), pp. 2319–2328

[26] Chen, W.L., Cheng, K.M., Chen, K.F.: 'Derivation and verification of a vector controller for induction machines with consideration of stator and rotor core losses', *IET Electr. Power Appl.*, 2018, **12**, (1), pp. 1–11

[27] Levi, E.: 'Impact of iron loss on behavior of vector controlled induction machines', *IEEE Trans. Ind. Appl.*, 1995, **31**, (6), pp. 1287–1296

[28] Levi, E., Sokola, M., Boglietti, A.*, et al.*: 'Iron loss in rotor-flux-oriented induction machines: identification, assessment of detuning, and compensation', *IEEE Trans. Power Electron.*, 1996, **11**, (5), pp. 698–709

[29] Matsuse, K., Yoshizumi, T., Katsuta, S.*, et al.*: 'High-response flux control of direct-field-oriented induction motor with high efficiency taking core loss into account', *IEEE Trans. Ind. Appl.*, 1999, **35**, (1), pp. 62–69

[30] Qu, Z., Ranta, M., Hinkkanen, M.*, et al.*: 'Loss-minimizing flux level control of induction motor drives', *IEEE Trans. Ind. Appl.*, 2012, **48**, (3), pp. 952–961

[31] Farasat, M., Trzynadlowski, A.M., Fadali, M.S.: 'Efficiency improved sensorless control scheme for electric vehicle induction motors', *IET Electr. Syst. Transp.*, 2014, **4**, (4), pp. 122–131